



Article

Mechanical and Numerical Assessment of Localized Soil Voids Under PCCP Joints

Haizhen Li ^{1,*}, Xin Feng ²  and Ankui Hu ¹ ¹ School of Energy and Power Engineering, Xihua University, Chengdu 610039, China² Faculty of Infrastructure Engineering, Dalian University of Technology, Dalian 116024, China

* Correspondence: lhzen@mail.xhu.edu.cn

Abstract: Uniform support from the surrounding soil is important for maintaining the stable operation of buried pipelines. For segmented prestressed concrete cylinder pipe (PCCP), localized soil voids around the joint due to leakage or engineering activities make the pipe unsupported partially and threaten its integrity and strength. In this paper, the impact of a localized soil void on a pipe joint is qualitatively assessed using a beam-on-elastic-spring approximation model. It further provides quantitative analysis through a nonlinear finite element (FE) model of PCCPs and the surrounding soil. The derived algebraic solutions indicate that a unilateral local void induces shear force and rotation at the joint, whereas shear force becomes negligible when the void spans the joint, leading to increased rotation. Moreover, the rotation angle shows a positive correlation with soil load and a negative correlation with pipe diameter. Numerical analysis reveals that void elongation along the pipe length has a more pronounced effect on structural response than void depth and angle. When the void length reaches 2.5 m, the maximum principal stress on the mortar layer of the PCCP increases approximately eight-fold compared to the scenario without voids. Due to the rigidity and safety factor of the PCCP, small voids in the bedding typically do not cause immediate pipe damage or joint leakage; however, they can significantly alter the stress distribution within both the pipe and surrounding soil. As the void develops, the soil may collapse and compromise support, leading to additional secondary disaster risks and potential threats to pipeline safety. This research emphasizes the importance of effective pipe-soil interactions and provides theoretical insights for developing repair strategies for PCCP.



Citation: Li, H.; Feng, X.; Hu, A. Mechanical and Numerical Assessment of Localized Soil Voids Under PCCP Joints. *Buildings* **2024**, *14*, 3624. <https://doi.org/10.3390/buildings14113624>

Academic Editor: Harry Far

Received: 27 July 2024

Revised: 22 October 2024

Accepted: 11 November 2024

Published: 14 November 2024



Copyright: © 2024 by the authors. Licensee MDPI, Basel, Switzerland. This article is an open access article distributed under the terms and conditions of the Creative Commons Attribution (CC BY) license (<https://creativecommons.org/licenses/by/4.0/>).

Keywords: prestressed concrete cylinder pipe; bell and spigot joint; soil void; theoretical method; FE analysis

1. Introduction

The underground pipeline system is crucial for meeting essential material needs in daily life and industrial production. Ensuring the structural safety of buried pipelines, including detection, maintenance, and management for long-term safe operation, is a significant challenge that primarily depends on two factors: structural integrity and effective soil-pipe interaction [1]. Furthermore, the two factors are interdependent. Uneven foundation conditions can lead to reduced support for buried pipelines, resulting in structural damage to the pipes [2,3]. Additionally, pipe damage, such as leakage and cracking, can erode the underlying soil, further compromising soil stability [4]. It has been reported that failures in underground pipelines are a leading cause of urban road collapse accidents [5]. However, substantial attention has traditionally been focused on the structural strength and integrity of pipelines, often based on the assumption of uniform bedding [6].

During the service life, pipelines often experience non-uniform longitudinal soil support due to various factors. In fact, the non-uniform bedding support can induce cracks or local subsidence of buried pipe, thereby diminishing structural-bearing capacity [7,8]. Consequently, there is growing attention to analyzing the damage and risks to pipeline

structures posed by non-uniform soil-pipe interaction including local voids [9,10]. Voids around underground pipelines are generally caused by internal factors or non-structural external factors [11]. External causes include groundwater or engineering activities that wash away finer particles from loosely filled soil, leading to erosion voids as water infiltrates and transports these particles downstream. Internal causes primarily stem from improper installation or structural damage due to aging, overload, or adverse conditions, manifesting as drips, leaks, and seepage. These issues cause continuous infiltration and erosion of soil particles, forming voids around the pipeline. For rigid pipelines, the loss of soil support due to such voids reduces resistance and affects pipe-soil interaction. Talesnick and Baker [12] reported a void at the pipe invert during excavation, observing a significant gap. Additionally, economical and effective repair technologies for the defects around the pipe have been proposed to prevent greater failures and consequences [13–15].

Prestressed Concrete Cylinder Pipe (PCCP), shown in Figure 1, is an indispensable component in water supply networks and is extensively utilized in trans-regional water diversion projects. Due to the characteristics of large diameter and pressure water delivery, the consequences will be disastrous and catastrophic once failure occurs. Moreover, it is a composite segmented pipeline consisting of concrete, mortar, steel cylinder, and prestressing wires (see Figure 2), with the steel wires serving as the primary load-bearing component. Once cracks appear in the mortar, it can provide conditions for external corrosive substances to contact the prestressed steel wire, posing a serious threat to operational safety and service life [16]. As long-span buried pipelines, PCCPs may experience uneven pipe-soil interaction due to local voids caused by internal or external factors during their service [17]. Case studies also have demonstrated that a reduction in longitudinal pipe-soil interaction in segmented buried pipelines can lead to more severe failure consequences [18–21]. However, current PCCP design and research often assume a uniform foundation, primarily focusing on the structural response of pipes buried in uniform bedding [22]. The response under uneven support conditions has received relatively little attention. Additionally, the spigot-and-bell joint is particularly vulnerable to damage due to uneven support, which can generate shear forces and angular stresses at the joint, leading to cracks or leaks. This can result in the pipeline reaching its service life prematurely, even before the structural strength is compromised. Therefore, it is essential to analyze the response and damage to segmented PCCP under uneven foundation conditions to inform prospective and preventive technology development.



Figure 1. Prestressed Concrete Cylinder Pipe.

In this study, the cause and potential harm of a local void around the buried pipeline are analyzed first. It then conducts a comparative qualitative analysis to assess the influence of the void position on shear and rotation angle using the beam-on-elastic-spring approximation model. Based on the results, the finite element model of the PCCP with a local soil void is developed to quantitatively evaluate the pipe response and material damage. This study aims to evaluate the impact of uneven pipe-soil interaction (localized void) on buried PCCP, and the findings could provide a foundation for assessing structural safety throughout their lifecycle.

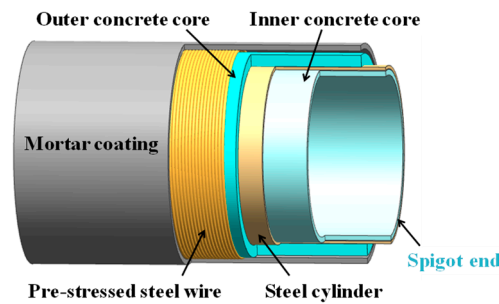


Figure 2. Schematic diagram of composited PCCP.

2. Mechanical Analysis

The presence of soil voids results in localized loss of support and alters the original stress distribution in the pipeline-soil interaction. Specifically, voids beneath pipe joints can induce shear forces and rotational effects. In this section, the expressions of shear force and rotation angle with unilateral and bilateral voids are derived, respectively, using the mechanical beam-on-elastic-spring approximation model [23]. The model considers two rigid pipes with rigidity significantly greater than the stiffness of the surrounding soil, connected by the moment-release joint. Shear forces develop to ensure that the vertical deformations of the two pipes at the joint remain consistent. A qualitative analysis investigates the impact of parameters such as void location, length, soil stiffness, and pipe diameter.

2.1. Analysis Model

(1) Unilateral void

The support and response diagram of a unilateral local soil void on the pipe joint is shown in Figure 3. The physical balance and moment balance equation of the pipe with a unilateral soil void are established as follows:

$$\begin{cases} F_L = kdl_1u_L \\ F_R = kdlu_R \end{cases} \quad (1)$$

$$\begin{cases} F_L e_L = \frac{1}{2}kd\theta_L \frac{1}{2}l_1 \frac{1}{2}l_1 \frac{2}{3} \frac{1}{2}l_1 \times 2 \\ F_R e_R = \frac{1}{2}kd\theta_R \frac{1}{2}l \frac{1}{2}l \frac{2}{3} \frac{1}{2}l \times 2 \end{cases} \quad (2)$$

where k is soil stiffness; l and d is the pipe length and outside diameter, respectively; u_L, u_R is vertical displacement under vertical force load (F_L, F_R); l_0 ($l_0 = l - l_1$) is void length.

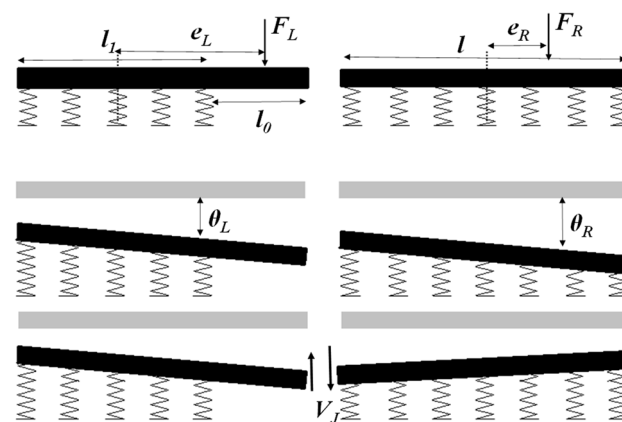


Figure 3. Longitudinal force and response sketch of pipe with a unilateral soil void.

Then, the vertical displacement at the center of the pipe can be obtained as follows:

$$\begin{cases} u_L = \frac{F_L}{kdl_1} \\ u_R = \frac{F_R}{kdl} \end{cases} \quad (3)$$

According to the moment balance equation, the respective joint angle (θ_L, θ_R), and the respective vertical displacement ($\Delta u_L, \Delta u_R$) of the joint without taking into account the interactions can be obtained as follows:

$$\begin{cases} \theta_L = \frac{12F_L e_L}{kdl_1^3} \\ \theta_R = \frac{12F_R e_R}{kdl^3} \end{cases} \quad (4)$$

$$\begin{cases} \Delta u_L = \theta_L \left(l_0 + \frac{1}{2}l_1 \right) \\ \Delta u_R = \theta_R \frac{1}{2}l \end{cases} \quad (5)$$

If the response of two beams is independent, the relative vertical movement of the joint is as follows:

$$u_J = u_L + \Delta u_L - (u_R - \Delta u_R) \quad (6)$$

(2) Void spanning the joint

When the void spans the joint (the void longitudinal length is both l_0), the schematic of soil local support and the mechanical response is shown in Figure 4. The physical balance and moment balance equations are established as Equations (7) and (8), and the derivation of displacement and rotation angle is similar to the unilateral void mentioned above.

$$\begin{cases} F_L = kdl_1 u_L \\ F_R = kdl_1 u_R \end{cases} \quad (7)$$

$$\begin{cases} F_L e_L = \frac{1}{2}kd\theta_L \frac{1}{2}l_1 \frac{1}{2}l_1 \frac{2}{3} \frac{1}{2}l_1 \times 2 \\ F_R e_R = \frac{1}{2}kd\theta_R \frac{1}{2}l_1 \frac{1}{2}l_1 \frac{2}{3} \frac{1}{2}l_1 \times 2 \end{cases} \quad (8)$$

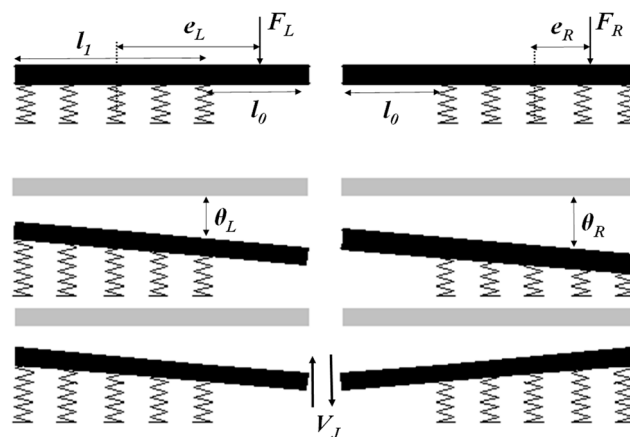


Figure 4. Longitudinal force and response sketch with a void spanning the joint.

2.2. Shear Force and Rotation

When the relative displacement occurs between the spigot and bell end, the shear forces V_J and the relative rotation angle θ_J of the joint occur. Regardless of the gasket deformation, the shear force is to eliminate most of the net shear displacement of the joint, that is, $u_J + \Delta u_J = 0$. The incremental deformations of the beam resulting from shear can be calculated using the following Equations (3)–(6), where $F_L = -V_J, e_L = l_0; F_R = V_J, e_R = -1/2l$.

Therefore, the shear force with a unilateral soil void can be evaluated from

$$\Delta u_J = - \left(\frac{V_J}{kdl_1} + \frac{12V_J \left(\frac{1}{2}l_0 + l_0 \right)^2}{kdl_1^3} + \frac{4V_J}{kdl} \right) \quad (9)$$

$$V_J = u_J \cdot A^{-1} \quad (10)$$

where $A = \frac{1}{kdl_1} + \frac{12(l_0+l_1/2)^2}{kdl_1^3} + \frac{4}{kdl}$.

Similarly, the relative rotation angle θ_J is the difference between load angle and shear angle.

$$\theta_J = \theta_L - \theta_R + \Delta\theta_L - \Delta\theta_R \quad (11)$$

$$\theta_J = \frac{12F_L e_L}{kdl_1^3} - \frac{12F_R e_R}{kdl^2} + \frac{-12V_J(l_0 + 1/2l_1)}{kdl_1^3} + \frac{6V_J}{kdl^2} \quad (12)$$

Considering the uniform load is caused by backfill over the pipes, $F_L = F_R = ql = q(l_1 + l_0)$, the values for joint shear and rotation for uniform length under the case of the unilateral soil void become

$$\begin{cases} V_J = qlA^{-1}B \\ \theta_J = \frac{6ql}{kd} \left[\frac{l_0}{l_1^3} - A^{-1}B \left(\frac{2l_0+l_1}{l_1^3} - \frac{1}{l^2} \right) \right] \end{cases} \quad (13)$$

where $A = \frac{1}{l_1} + \frac{12(l_0+1/2l_1)^2}{l_1^3} + \frac{4}{l}$, $B = \frac{1}{l_1} - \frac{1}{l} + \frac{6l_0^2+3l_0l_1}{l_1^3}$.

Repeating the process above, the expressions with void spanning the joint can be derived by

$$\begin{cases} V_J = 0 \\ \theta_J = \frac{ql}{kd} \cdot \frac{12l_0}{l_1^3} \end{cases} \quad (14)$$

According to Equations (13) and (14), the shear of the buried rigid pipeline with unilateral void is related to three factors, namely, the void length, the pipe length, and the overlying load (see Figure 5a). Additionally, the relative rotation angle of the joint is also influenced by pipe diameter and foundation stiffness, besides the above factors. Both shear force and rotation angle are positively correlated with the overlying load. When the void spans the joint symmetrically, the shear force is zero, but the rotation angle is greater compared to a unilateral void and negatively correlated with the pipe diameter (as shown in Figure 5b).

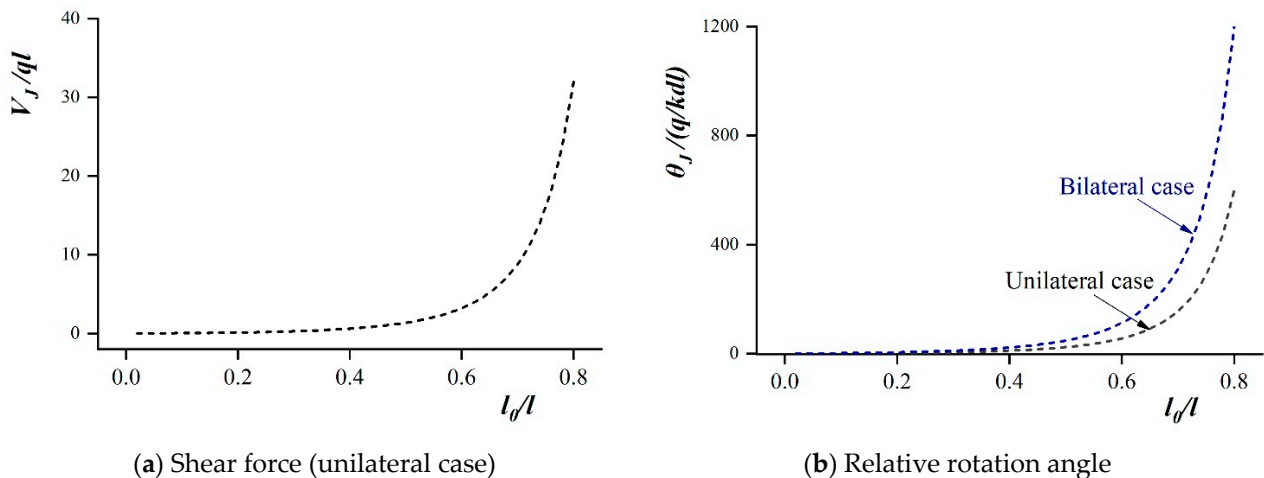


Figure 5. (a) Shear force and (b) relative rotation angle on the joint with local soil void.

Since the relative rotation angle of the joint serves as a critical safety indicator for segmented pipelines, longitudinal non-uniform support caused by a local void spanning the joint is relatively unfavorable. PCCP pipelines are segmented with rigid pipes connected by flexible joints; therefore, the qualitative assessment results above serve as a reasonable reference. To quantitatively analyze the impact of a localized soil void on stress response and materials damage to PCCP, an FE simulation model including pipes and the surrounding soil was developed in the following section.

3. Numerical Analysis

In this section, the size effect of local void is investigated by establishing a buried PCCP nonlinear finite element model considering the pipe-soil interaction. Based on the pipe damage and soil failure results, the response characteristics of the buried PCCP under local soil voids are further summarized.

3.1. Finite Element Modeling

As known above, the adjacent buried pipes with a void spanning the joint can lead to a larger relative rotation angle, representing a more unfavorable condition. Moreover, the joint is prone to seepage and even leakage in adverse conditions, forming a void. Because of the difficulty of a void geometry measurement, a simple shape that is easy to simulate is used to study the influence based on the assumptions of previous scholars in numerical modeling [3,24,25]. In this study, void angle (VA), void depth (VD), and void length (VL) are used as the dimension control parameters, as shown in Figure 6. To study parameter sensitivity, the void angles are set as 20°, 40°, 60°, and 90°, with void depths of 50 and 100 and void lengths of 62, 125, and 250. For the convenience of expression, the format of the void size defined in this section is VA (°)-VD (mm)-VL (cm). The birth-death element technology in finite element is a common method in structural engineering simulation for the simulation of drilling, excavation, backfilling, and other processes, which deactivate or reactivate specific regions/sets through model changes. Therefore, the formation and evolution process of the void is simulated by the birth-death element method.

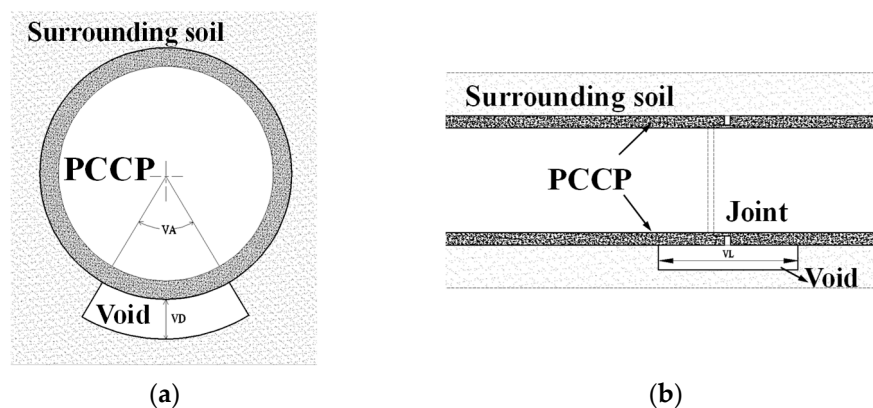


Figure 6. Sketch of soil void: (a) cross-section and (b) vertical-section.

Based on the nonlinear analysis software ABAQUS2019, the finite element model of two adjacent PCCPs, including the bell-and-spigot joint, and their surrounding soil were assembled, as depicted in Figure 7. The key parameters for the embedded PCCP were as follows: burial depth $H = 2.5$ m, inside diameter $D = 3.8$ m, work pressure $P = 0.6$ MPa, and single pipe length $L = 5$ m. The section was modeled with five layers, and the interactions between adjacent layers make them work together. The concrete core, mortar, and surrounding soil were modeled using an eight-node reduced-integration “brick” element (C3D8R), while a four-node reduced-integration shell element (S4R) was used for the steel cylinder. To account for the stiffness contribution of the steel wire, a two-node truss element (T3D2) was employed for the prestressed steel wire, and the equivalent

cooling method was used to simulate the prestress [26]. The stress-strain relationships of PCCP are derived from the current AWWA C304 standards [27], and the strain damage threshold is $1155 \mu\epsilon$ for mortar. The material parameters of the PCCP and the surrounding soil are shown in Tables 1 and 2. The pipe-pipe interaction was modeled using the contact mechanics method, which employs a contact algorithm to describe interface friction. A fully bonded interface was assumed for the pipe-soil interaction, achieved by defining a tie constraint. [7]. In addition, the other finite element implementation adheres to the process outlined in the published paper [28]. The whole model comprises about 240,000 elements and 270,000 nodes.

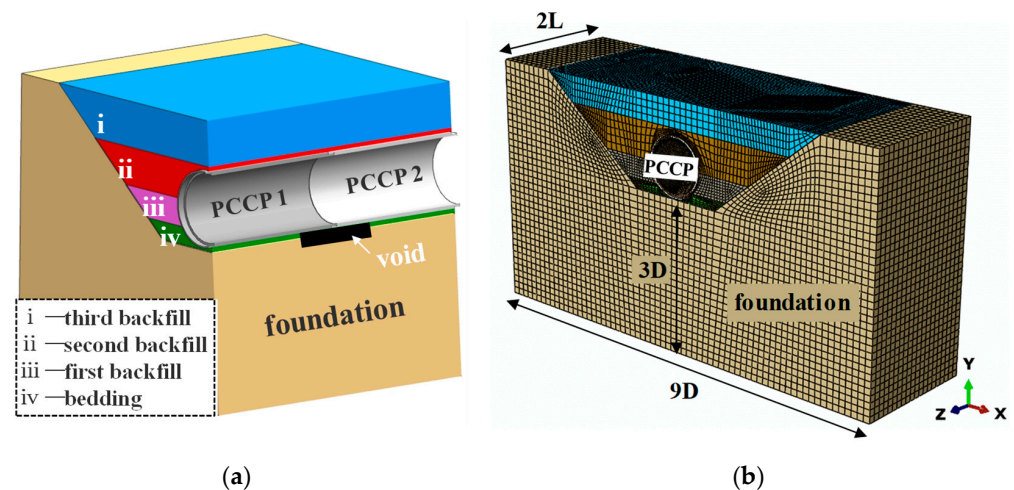


Figure 7. Sketch of the PCCPs: (a) half the buried pipes and (b) the whole model after meshing.

Table 1. Material parameters of PCCP.

Component	Density (kg/m^3)	Young's Modulus (MPa)	Poisson's Ratio	Compressive Strength (MPa)	Tensile Strength (MPa)
Prestressing wires	7833	205,000	0.3	1570	1570
Concrete	2500	35,500	0.2	35.5	2.74
Steel cylinder	7833	206,000	0.3	235	235
Mortar coating	2200	24,165	0.2	45	3.49

Table 2. Material parameters of the soil.

Soil Layer	Density (kg/m^3)	Young's Modulus (MPa)	Poisson's ratio	Cohesion (kPa)	Friction Angle ($^\circ$)
Natural foundation	1890	80	0.25	5	30
Bedding	2200	40	0.29	3	30
Backfill	2000	50	0.35	4	30

Twelve steps were performed to simulate the state of the pipeline during operation (gravity of the backfills, pipe, and fluid, operating internal pressure, and the effect of groundwater), and then the soil void was introduced. Three types of boundary conditions were implemented as follows: the bottom of the model was fixed in three directions, the top surface was left unconstrained to act as a free surface, and the remaining four surfaces were restrained against displacement in their normal directions.

3.2. Pipe Stress Analysis

The local void in the bedding results in uneven support, altering the interaction between the pipe and soil and consequently affecting pipe stress. Figure 8 shows the

influence of the void on the maximum principal stress of the mortar layer at various characteristic positions along the lateral longitudinal path. Under operational loads, the overall PCCP deformation is “elliptical”. The maximum principal stress at the pipe waist is markedly higher than that at the crown and invert, and the value is about 3.5 MPa, 1.0 MPa, and 0.2 MPa, respectively, with minimal variation along the longitudinal path. The introduction of a local void (20-100-125) causes the redistribution of pipe stress and has an obvious effect on the pipe invert. Its influence gradually decreases along the longitudinal path, while the maximum principal stress increases by about 1.1 MPa. In other words, the increase can lead to the tensile state of the mortar and concrete, which may result in damage to the pipe material.

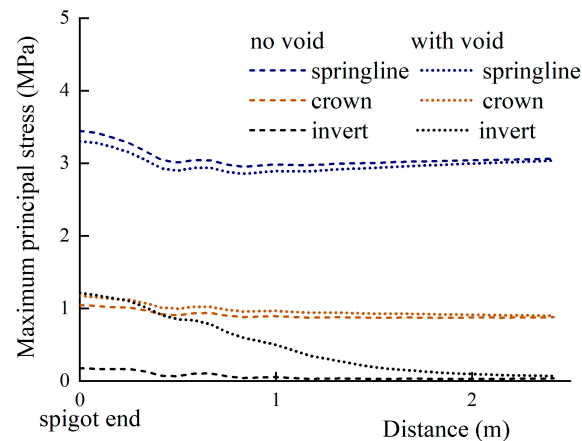


Figure 8. Effect of a void on the maximum principal stress of the pipe (longitudinal path).

As seen in Figure 8, the most vulnerable location in a local void is the pipe invert. In order to evaluate the impact of void evolution on pipe stress, the maximum principal stress is extracted for varying void sizes, as illustrated in Figure 9. The presence of a local void in the bedding results in an increase in the maximum principal stress at the pipe end (above the void), with the increment gradually decreasing along the longitudinal direction away from the void. The size of the void has a significant effect on the maximum principal stress, with void length exerting a greater impact compared to the depth and angle. A longer void length results in a larger longitudinal response range. When the VL reaches 2.5 m, the maximum principal stress increases by approximately 8 times compared to the case with no void.

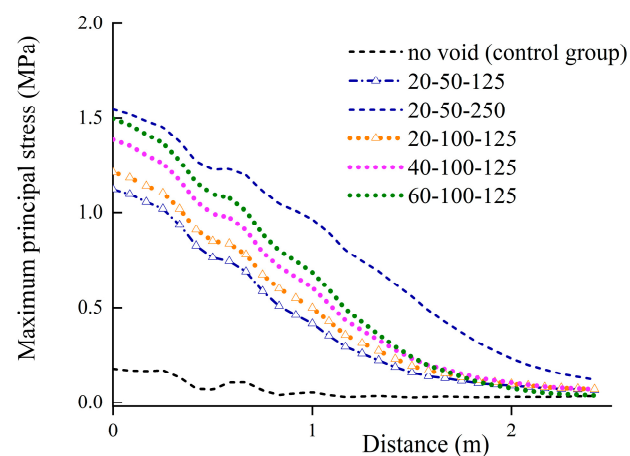


Figure 9. Effect of a void size on the maximum principal stress on the pipe invert.

Figure 10 shows directional stresses in the mortar layer of the outer middle section, comparing conditions without and with a soil void (void size: 20-100-125). The axial

stress is uniformly distributed along the circumferential path and less affected by the void. The circumferential stress is basically equal to the maximum principal stress; that is, the direction of maximum principal stress is circumferential. Under the void condition, the maximum principal stress at the pipe invert increases by approximately 0.78 MPa, resulting in tensile stress. Therefore, it is essential to further investigate the material damage to the mortar layer. Additionally, the presence of a void significantly increases the circumferential stress, which is consistent with the field test results on concrete pipes [15].

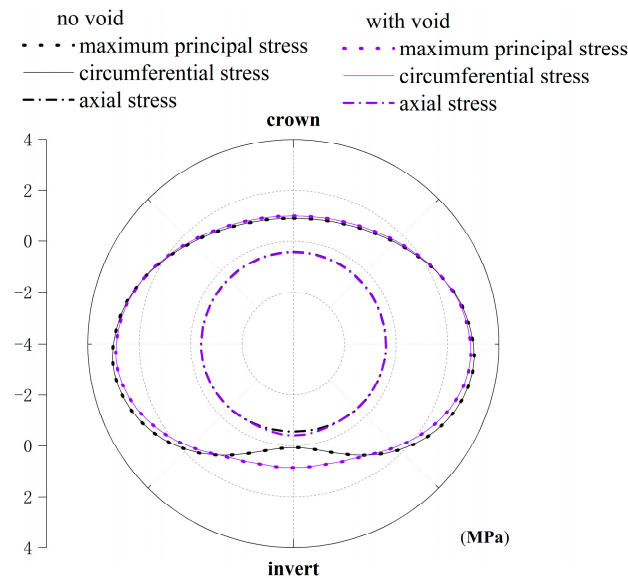


Figure 10. Effect of a void on the stress of the pipe outside surface (circumferential path).

Differing from the mortar, the maximum principal stress of the concrete core is basically equal to the axial stress, indicating that the direction of the maximum principal stress is axial and evenly distributed along the path. Figures 11 and 12 illustrate the impact of a void on concrete stress at the spigot and bell ends, respectively. The concrete core experiences circumferential compression due to prestressing. The compressive stress resulting from prestressing is greater than the circumferential stress under the operation loads, maintaining a compressive state in circumferential stress.

The void primarily affects the circumferential stress of the concrete core, reducing the circumferential compressive stress by approximately 0.9 MPa at the outer side of the pipe invert (see Figure 11a) and by 0.6 MPa at the spigot and bell ends (see Figure 12a). The circumferential distribution on the inner is opposite to that on the outer path. The circumferential compressive stress at the invert of the inner concrete increases because of the void, with rises of about 0.7 MPa at the spigot (see Figure 11b) and 0.8 MPa at the bell end (see Figure 12b). Notably, the maximum principal stress of the inner spigot end (Figure 11b) and the outer bell end (Figure 11a) is tensile. The value of the inner spigot end is about 2.4 MPa, but it does not reach the tensile strength of the concrete. In conclusion, the soil void affects the circumferential stress of the concrete core, which remains compressive. Namely, the void does not cause crack damage to the concrete but rather alters its stress distribution. The potential damage to the material is mainly the crack of the mortar protective layer.

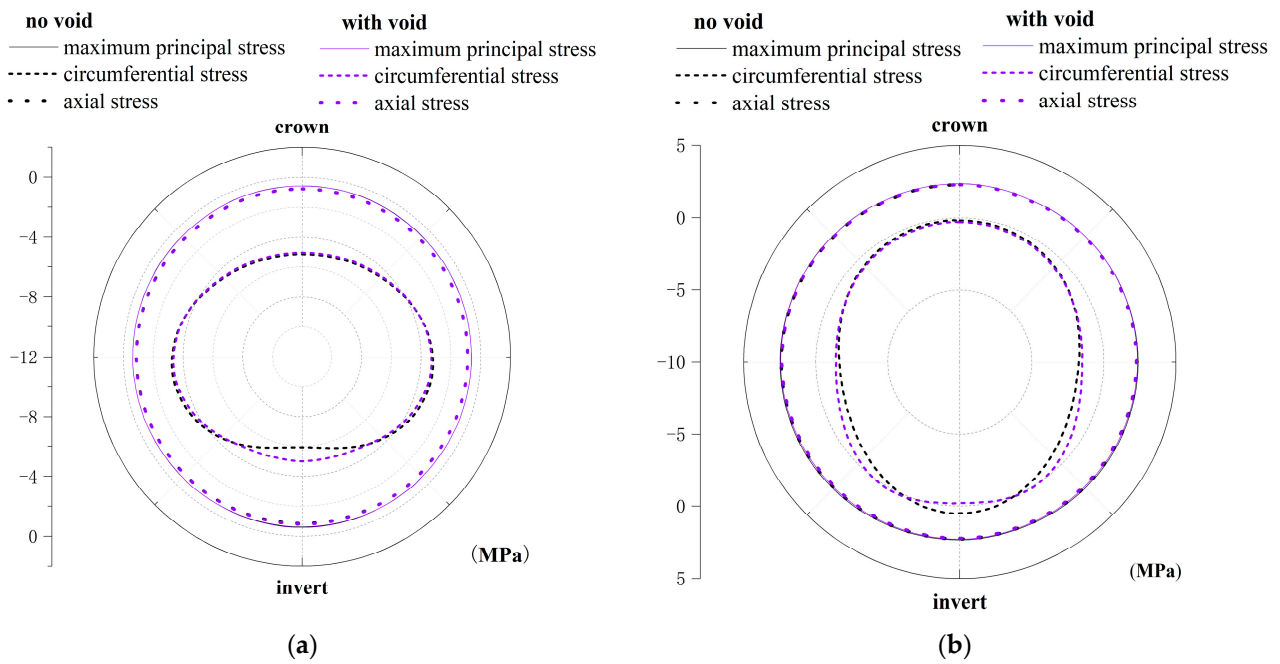


Figure 11. Effect of a soil void on the stress of the concrete at pigot end: (a) outside and (b) inside.

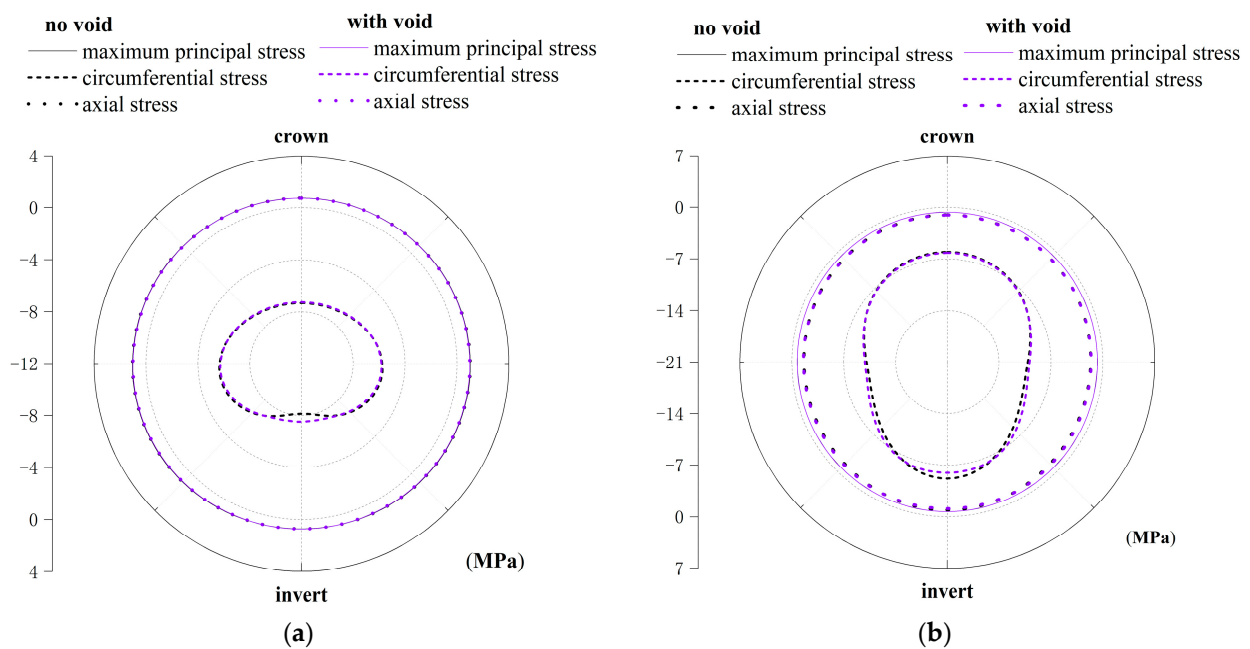


Figure 12. Effect of a soil void on the stress of the concrete at bell end: (a) outside and (b) inside.

The soil void spanning the joint causes a change in the stress state of the pipe, including a redistribution of the bending moment in the concrete core. The formation of local voids leads to a decrease in the bending moment at critical positions, which is consistent with the findings in the published literature (see Figure 13 below). Figure 14 further compares the influence of void size (length, depth, and angle) on the bending moment along the circumferential path. The greatest impact is observed at the pipe invert, where the maximum reduction is approximately 70%. Furthermore, the void depth and angle have a lesser influence on the bending moment than the void length. As the length of the void increases, the bending moment of the concrete gradually increases at the pipe invert.

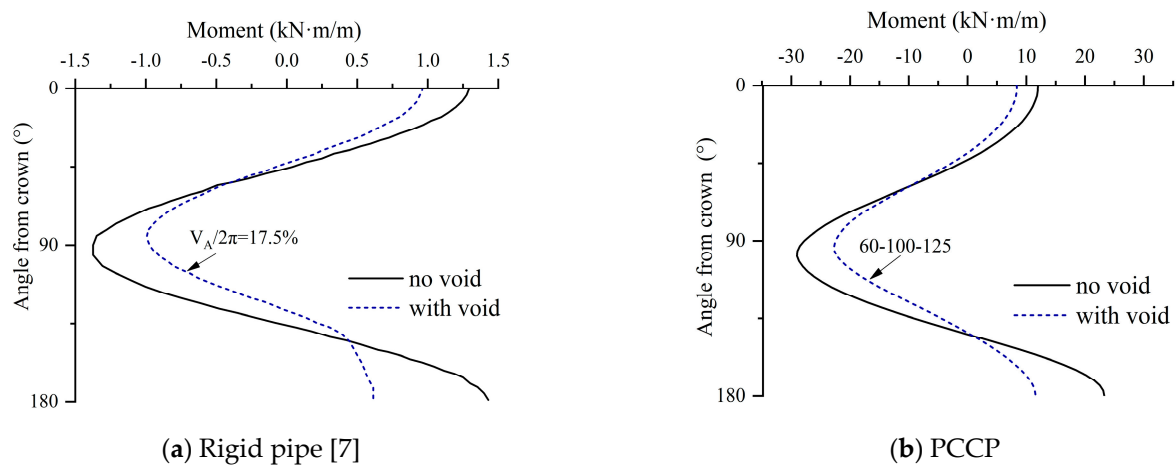


Figure 13. Effect of void at pipe invert on the moment: (a) rigid pipe and (b) PCCP.

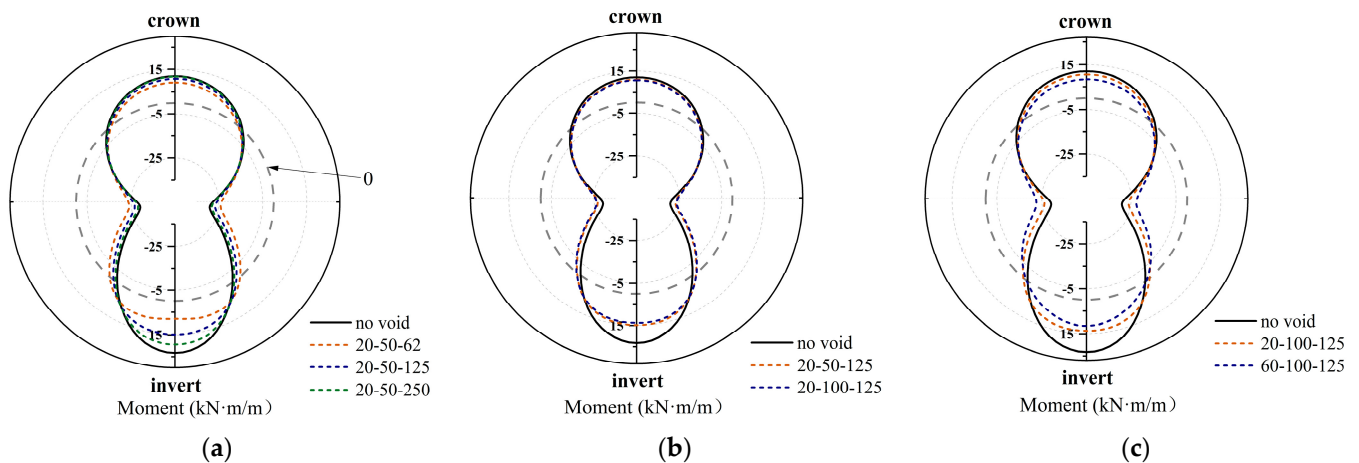


Figure 14. Effect of void size on the moment of the concrete at bell end: (a) VL, (b) VD, and (c) VA.

3.3. Joint Angle and Material Damage

The vertical displacement of the pipeline is about 1.3 cm under operational loads. During service, adverse operational conditions may create localized ground voids, causing unsupported soil and subsequent pipe displacement. Figure 15 shows the vertical displacement of pipe with different soil void sizes. It is evident that the void causes vertical displacement, and the closer to the void, the greater the displacement. When the void is 20-100-125, the maximum vertical displacement of joint reaches about 1.33 cm. With the continuous expansion, the vertical displacement increases, and the displacement increases to about 1.38 cm when the void evolves to 90-100-125. Consequently, the local soil void in the bedding can cause vertical displacement of the pipe, while the displacement due to void is quite small and can be ignored for large-diameter PCCP.

The joint is the relatively weak position of the segmented pipeline. A local soil void spanning the joint can cause the vertical displacement of the pipe on longitudinal path, resulting in the relative angle of the pipe joint. Figure 16 illustrates the effect of void size on the relative angle. As void evolution (increasing in angle, length, and depth), the relative angle of the pipe joint tends to increase continuously. However, the maximum angle observed is approximately 0.02° , which maintains a significant safety margin relative to the permissible angle limit of 0.5° [29]. Thus, a small local void does not significantly alter the joint angle, indicating a low risk of leakage due to the localized void.

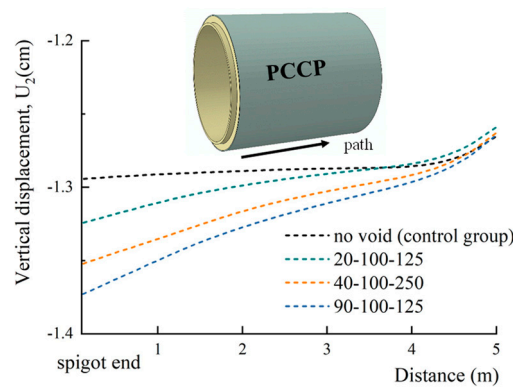


Figure 15. The vertical displacement of the pipe under a soil void.

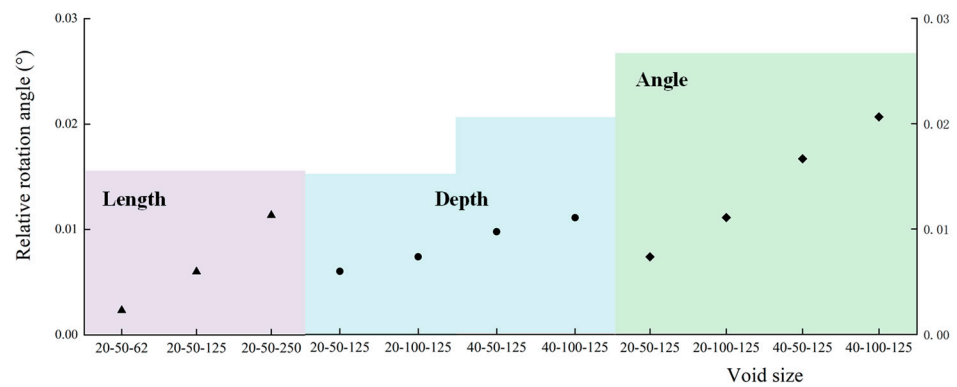


Figure 16. Effect of void sizes on the relative angle of jointed PCCPs.

PCCP is a composite material pipe, and the cracks on the mortar layer and concrete are the initial signs of pipe damage. The maximum principal strain of the mortar with (the void size is 20-50-250) and without (operation condition) void is shown in Figure 17. The PCCP exhibits an “elliptic” deformation under operational loads, with the maximum principal strain of the mortar layer measuring approximately $160 \mu\epsilon$ at the pipe springline and about $10 \mu\epsilon$ at the pipe invert. The local void changes the stress state of the pipe, and the maximum principal strain slightly increases to about $165 \mu\epsilon$ and $60 \mu\epsilon$ at the waist and invert, respectively. The values remain significantly below the specified limit for mortar crack damage [27].

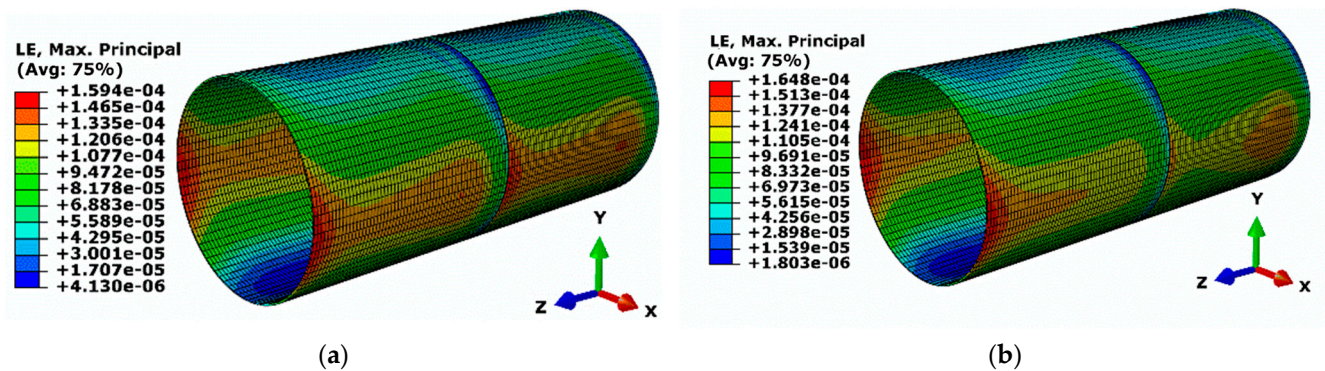


Figure 17. Maximum principal strain of the mortar coating: (a) operation and (b) local void (20-50-250).

To sum up, due to the design safety factor and the large rigidity of the large-diameter PCCP, the local void (with a maximum size of 90-100-250) has little influence on the vertical

displacement and relative angle for large PCCP. Consequently, the risk of leakage from excessive angle changes or significant material cracking induced by local voids is low. This further indicates that large PCCP has good structural safety and can withstand local ground inhomogeneity in a certain range.

3.4. Influence of Local Void on Soil Stability

To analyze the stability state of soil around the void, the Molar-Coulomb nonlinear constitutive relationship model is employed, and its shear failure criterion can be expressed as follows:

$$\tau > \tau_f = c + \sigma \tan \varphi \quad (15)$$

where τ is shearing stress, τ_f is the critical shear strength of soil is determined by cohesion c and internal friction angle φ .

According to the relationship between normal stress and shear stress, the strength theory expressed by the maximum principal stress can be derived as follows:

$$\sigma_1 > \sigma_{1f} = \frac{1 + \sin \varphi}{1 - \sin \varphi} \cdot \sigma_3 + 2c \frac{\cos \varphi}{1 - \sin \varphi} \quad (16)$$

Then, a constant SF for shear failure is defined in post-processing, $SF = \sigma_{1f} - \sigma_1$, that is, the soil is shear failure when $SF < 0$. Figure 16 shows the nephogram of bedding soil under three cases: operational load (no void), void formation (20-50-62), and expansion (20-100-125). Under operational loads (Figure 18a), the bedding soil is evenly stressed with no shear failure occurring. When the soil void appears, the bedding can no longer provide uniform support, resulting in a change in stress state and approaching the shear critical value at the pipe waist (Figure 18b). The soil at the pipe waist and on both sides of the void has shear failure when the void continues to enlarge in size, as shown in Figure 18c. Therefore, the soil state around the void is influenced by its size, with larger voids posing a greater risk of collapse. Additionally, loose soil is prone to loss, which can exacerbate void expansion, weaken the interaction between the pipe and soil, and jeopardize pipeline safety.

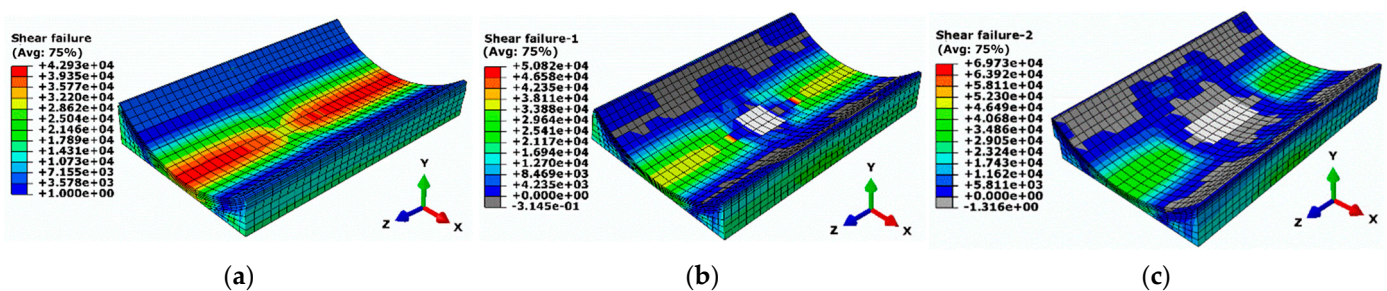


Figure 18. Shear failure nephogram of the bedding soil: (a) operation condition, (b) void production, and (c) void evolution.

In summary, the large stiffness and high safety factor of a PCCP ensure that a small local void in the bedding does not typically lead to severe material damage to the pipe itself. However, it does significantly alter the stress distribution within both the pipe and the surrounding soil. As voids evolve, there is an increased risk of the mortar protective layer cracking. Moreover, the support loss due to void and the secondary damage from soil collapse are the main potential threats to the safe operation of the pipeline. Therefore, timely measures, such as grouting, are essential to prevent more serious consequences.

4. Conclusions and Recommendations

Ensuring stable pipe-soil interaction is crucial for the safe operation of buried pipelines. Soil voids can lead to uneven support, which is an unavailable condition for buried segmented PCCPs. This paper derives expressions for the shear force and rotation angle of

a joint under a local void using a beam-on-elastic-spring approximation model. It then qualitatively assesses the influence of parameters such as soil stiffness, pipe length, pipe diameter, and void length. Based on the results, a nonlinear three-dimensional numerical model was developed to investigate the effects of bedding voids on the stress state and material damage to large buried PCCPs in service. The evaluation facilitates the prevention of functional failures and contributes to the longevity of the pipeline. The main conclusions are as follows:

(1) For rigid pipelines, a unilateral local void induces shear force and rotation angle, and the shear force is related to void length, pipe length, and overburden load. Symmetric bilateral void results in zero shear force but significantly increases the rotation angle, which is positively correlated with overburden load and negatively correlated with the pipe diameter.

(2) The local void alters the pipe-soil interaction, primarily impacting circumferential stress while having a lesser effect on axial stresses in the mortar layer of PCCP. Compared to void depth and angle, void elongation in the longitudinal direction has a more pronounced effect on pipe stress. When the void length reaches 2.5 m, the maximum principal stress increases about eight times compared with the no-void condition. Additionally, the local void leads to a reduction in the bending moment on the concrete, with a maximum decrease of approximately 70% at the pipe invert. As the void evolves, shear failure of the surrounding soil occurs, leading to local displacement nearby and potential collapse towards the void, leaving the pipe waist unsupported. Furthermore, the loose backfilled soil at the pipe invert may contribute to the formation of a larger-scale void.

(3) For large-diameter PCCP, a localized soil void in the bedding is unlikely to cause severe damage to the pipe material or increase the risk of joint leakage due to the high stiffness and safety factors incorporated in the design. However, it significantly alters the stress conditions between the pipe and the soil. As the void continues to evolve, collapse of the surrounding soil may occur, leading to a loss of foundation-bearing capacity and subsequent damages that pose a primary potential threat to pipeline safety. Therefore, timely grouting repairs at the locations of voids are essential to mitigate these potential hazards.

Author Contributions: Methodology, H.L.; Software, H.L.; Formal analysis, A.H.; Investigation, H.L.; Data curation, A.H.; Writing—original draft, H.L. and A.H.; Writing—review & editing, X.F.; Visualization, H.L.; Project administration, X.F.; Funding acquisition, X.F. All authors have read and agreed to the published version of the manuscript.

Funding: This research was funded by National Natural Science Foundation of China (Grant No.52079024) and the Scientific Research Program for the Talent of XIHUA University (Grant No. RX2300000879).

Data Availability Statement: Data are contained within the article.

Conflicts of Interest: The authors declare no conflict of interest.

References

1. Moser, A.; Folkman, S. *Buried Pipe Design*, 3rd ed.; McGraw Hill: New York, NY, USA, 2008.
2. Balkaya, M.; Moore, I.D.; Sağlam, A. Study of non-uniform bedding due to voids under jointed PVC water distribution pipes. *Geotext. Geomembr.* **2012**, *34*, 39–50. [[CrossRef](#)]
3. Balkaya, M.; Moore, I.D.; Sağlam, A. Study of non-uniform bedding support under continuous PVC water distribution pipes. *Tunn. Undergr. Space Technol.* **2013**, *35*, 99–108. [[CrossRef](#)]
4. Shi, X.; Cao, Y.; Rong, C.; An, G.; Wang, H.; Cui, L. Influence of Pipeline Leakage on the Ground Settlement around the Tunnel during Shield Tunneling. *Sustainability* **2022**, *14*, 16802. [[CrossRef](#)]
5. Wang, K.; Zhang, J.; Gao, G.; Qiu, J.; Zhong, Y.; Guo, C.; Zhao, W.; Tang, K.; Su, X. Causes, Risk Analysis, and Countermeasures of Urban Road Collapse in China from 2019 to 2020. *J. Perform. Constr. Facil.* **2022**, *36*, 04022054. [[CrossRef](#)]
6. Huo, Y.; Goma, S.M.M.H.; Zayed, T.; Meguid, M. Review of analytical methods for stress and deformation analysis of buried water pipes considering pipe-soil interaction. *Undergr. Space* **2023**, *13*, 205–227. [[CrossRef](#)]
7. Meguid, M.A.; Kamel, S. A three-dimensional analysis of the effects of erosion voids on rigid pipes. *Tunn. Undergr. Space Technol.* **2014**, *43*, 276–289. [[CrossRef](#)]

8. El-Taher, M. The Effect of Wall and Backfill Soil Deterioration on Corrugated Metal Culvert Stability. Ph.D. Thesis, Queen's University, Kingston, ON, Canada, 2009.
9. Sonoda, Y.K.T.; Asao, H.; Morikami, H.; Ling, H.I. The influence of non-uniform bedding on the mechanical behavior of buried flexible pipe. In Proceedings of the Pipelines 2013: Pipelines and Trenchless Construction and Renewals—A Global Perspective, Fort Worth, TX, USA, 23–26 June 2013; pp. 1321–1329.
10. Moore, I.D. Assessment of Damage to Rigid Sewer Pipes and Erosion Voids in the Soil, and Implications for Design of Liners. In Proceedings of the 2008 No-Dig Conference and Exhibition, Dallas, TX, USA, 3–6 June 2008; pp. 1–10.
11. McDonald, S.E.; Zhao, J.Q. *Condition Assessment and Rehabilitation of Large Sewers*, 1st ed.; CRC Press: Boca Raton, FL, USA, 2001.
12. Talesnick, M.; Baker, R. Investigation of the Failure of a Concrete-Lined Steel Pipe. *Geotech. Geol. Eng.* **1999**, *17*, 99–121. [[CrossRef](#)]
13. Peter, J.M.; Moore, I.D. Effects of Erosion Void on Deteriorated Metal Culvert before and after Repair with Grouted Slip Liner. *J. Pipeline Syst. Eng. Pract.* **2019**, *10*, 04019031. [[CrossRef](#)]
14. Li, Z.; Tang, F.; Chen, Y.; Zou, X. Stability of the pipe-liner system with a grouting void surrounded by the saturated soil. *Eng. Struct.* **2019**, *196*, 109284. [[CrossRef](#)]
15. Li, B.; Wang, F.; Fang, H.; Yang, K.; Zhang, X.; Ji, Y. Experimental and numerical study on polymer grouting pretreatment technology in void and corroded concrete pipes. *Tunn. Undergr. Space Technol.* **2021**, *113*, 103842. [[CrossRef](#)]
16. Hassi, S.; Ebn Touhami, M.; Menu, B.; Benqlilou, H.; Ejbouh, A. Case Study of the Performance of Prestressed Concrete Cylinder Pipes in Northeastern Morocco. *J. Pipeline Syst. Eng. Pract.* **2022**, *13*, 05022002. [[CrossRef](#)]
17. Livingston, B.; Ojdrovic, R.; Powell, B. Forensic evaluation of PCCP failures: Green bay water utilities case study. In Proceedings of the Pipelines 2018: Condition Assessment, Construction, and Rehabilitation, Toronto, ON, Canada, 15–18 July 2018; pp. 362–370.
18. Bucu, J.; Emeriault, F.; Le Gauffre, P.; Kastner, R. Statistical and 3D numerical identification of pipe and bedding characteristics responsible for longitudinal behavior of buried pipe. In Proceedings of the Pipelines 2006: Service to the Owner, Chicago, IL, USA, 30 July–2 August 2006; pp. 1–10.
19. Sheldon, T.; Sezen, H.; Moore, I.D. Joint Response of Existing Pipe Culverts under Surface Live Loads. *J. Perform. Constr. Facil.* **2015**, *29*, 04014037. [[CrossRef](#)]
20. Emeriault, F.; Bucu, J.; Kastner, R. Full-Scale Experimental Determination of Concrete Pipe Joint Behavior and Its Modeling. *J. Infrastruct. Syst.* **2008**, *14*, 230–240. [[CrossRef](#)]
21. Davies, J.P.; Clarke, B.A.; Whiter, J.T.; Cunningham, R.J. Factors influencing the structural deterioration and collapse of rigid sewer pipes. *Urban Water* **2001**, *3*, 73–89. [[CrossRef](#)]
22. Ge, S.; Sinha, S. Failure Analysis, Condition Assessment Technologies, and Performance Prediction of Prestressed-Concrete Cylinder Pipe: State-of-the-Art Literature Review. *J. Perform. Constr. Facil.* **2014**, *28*, 618–628. [[CrossRef](#)]
23. Wang, Y.; Moore, I.D. Simplified design model for rigid pipe joints based on the two-pipe approximation. *Can. Geotech. J.* **2015**, *52*, 626–637. [[CrossRef](#)]
24. Jaganathan, A.P.; Allouche, E.; Simicevic, N. Numerical modeling and experimental evaluation of a time domain UWB technique for soil void detection. *Tunn. Undergr. Space Technol.* **2010**, *25*, 652–659. [[CrossRef](#)]
25. Meguid, M.A.; Dang, H.K. The effect of erosion voids on existing tunnel linings. *Tunn. Undergr. Space Technol.* **2009**, *24*, 278–286. [[CrossRef](#)]
26. Hu, B.; Fang, H.; Wang, F.; Zhai, K. Full-scale test and numerical simulation study on load-carrying capacity of prestressed concrete cylinder pipe (PCCP) with broken wires under internal water pressure. *Eng. Fail. Anal.* **2019**, *104*, 513–530. [[CrossRef](#)]
27. *ANSI/AWWAC304*; Standard for Design of Pre Stressed Concrete Cylinder Pipe. American Water Works Association: Denver, CO, USA, 2014.
28. Li, H.; Feng, X.; Chen, B.; Zhao, L. Damage evaluation of a PCCP joint with a localized soil void and broken wires. *Adv. Struct. Eng.* **2021**, *24*, 3133–3143. [[CrossRef](#)]
29. *GB/T19685*; Prestressed Concrete Cylinder Pipe. Standards Press of China: Beijing, China, 2017.

Disclaimer/Publisher's Note: The statements, opinions and data contained in all publications are solely those of the individual author(s) and contributor(s) and not of MDPI and/or the editor(s). MDPI and/or the editor(s) disclaim responsibility for any injury to people or property resulting from any ideas, methods, instructions or products referred to in the content.